**A TALE OF TWO STRATIGRAPHIES: FROM ALBA PATERA TO THE NORTHERN PLAINS.** A. T. Polit[1], R. A. Schultz, and R. Soliva, Geomechanics-Rock Fracture Group, Department of Geological Sciences and Engineering/172, University of Nevada, Reno, NV 89557-0138, [1]polita@mines.unr.edu.

**Summary:** We measure the along-strike throw of grabens on Alba Patera and compare their characteristics with those of the distal segments of the echelon grabens of Tantalus Fossae. Major differences exist in the fault populations and throw distributions of the two areas studied, indicating a change in the Martian stratigraphy between these two regions.

**Introduction:** Many observable properties of faults (e.g. along-strike throw distributions, spacing, and displacement-length scaling) are influenced by vertical fault restriction and properties of the surrounding rock [1-3]. These relations allow us to use faults to investigate the mechanical stratigraphy of Mars.

Previous work examined grabens to the south and east of Alba Patera (Ceraunius and Tantalus Fossae), using Viking Orbiter data, with the aim to understand shallow crustal discontinuities [4,5]. Assuming that the fault intersection depth corresponds to a crustal discontinuity, discontinuities were attributed to the base of the megaregolith or a strength contrast within it [4,5], and mechanical discontinuities between volcanic and other units [5].

The Tantalus Fossae grabens afford an opportunity to investigate the changes in the geologic sequence from Alba Patera across the transition into the northern plains. We use Mars Orbiter Laser Altimeter (MOLA) based DEMs gridded at 200 pixels/° [6] to take cross-strike profiles and measure the fault throw along the lengths of faults on Alba Patera as well as the distal segments of the echelon grabens of Tantalus Fossae. No previous studies have examined the complete throw distributions of the Tantalus Fossae grabens. We use standard displacement-discontinuity boundary element modeling [7,8] to calculate the surface displacement and match this to the cross-strike topography of grabens in order to quantify depths of faulting.

**Alba Patera:** A concentric set of grabens located on the eastern flank of Alba Patera belongs to the third stage of faulting as defined by Tanaka [9]. We identify two distinct regions of deformation within this area (**Fig. 1**), with one region (A) consisting of localized, coalesced basins, and the other (B) consisting of long, distributed grabens.

Region A has localized deformation in the form of several deep, coalesced grabens. The faults we examined from a coalesced graben range in length from 25 to 130 km. The throw distributions are somewhat flat-topped, with a maximum displacement of ~700m on the longest fault (**Fig. 2a**). The fault throw appears to scale linearly with the fault length such that the throw to length ratio is $\sim 5\times10^{-3}$. This shows that the faults are growing with a constant aspect ratio (fault length/fault height), indicating that they are probably not restricted at depth [2]. Our boundary element modeling results show a maximum faulting depth of ~12 km. Localized deformation, similar to what is observed in this region, usually occurs either when there is no barrier to increasing displacement accumulation on one fault or set of faults (i.e. there is no restriction) or when a ductile layer occurs beneath a brittle layer [10].

Region B contains distributed deformation, with a series of shallower grabens striking ~N-NE. The grabens are long and narrow, with throws on the graben-bounding faults that are generally no larger than 300 m. The throws are fairly constant and exhibit flat-topped distributions. Boundary element modeling of a cross-strike profile of one of the grabens indicates a faulting depth of ~6 km. This pattern of distributed deformation with flat-topped displacement distributions and relatively uniform throws demonstrates that these faults are probably restricted by a mechanical boundary [1,3].

**Transition to the Northern Plains:** We measured the throw distributions on the distal segments of the echelon grabens of Tantalus Fossae (centered at 60°N, 270°E). These are part of an evenly distributed popula-

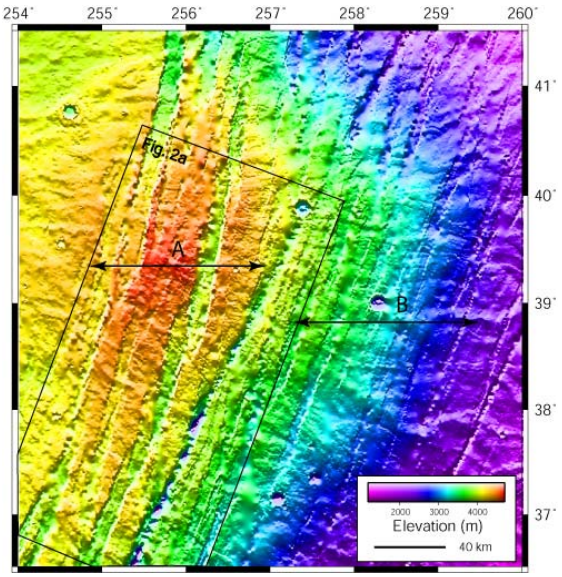


**Figure 1.** Shaded-relief DEM of the Alba Patera study area with regions A (localized deformation) and B (distributed deformation) labeled. Alba Patera summit is off the image to the left.

tion of long, narrow grabens that originate from the concentric grabens on the east flank of Alba Patera. We find a transition from peaked to flat-topped throw distributions as a function of length, with faults between 60 and 110 km in length exhibiting flat-topped distributions with approximately constant throws between 35 and 40 m (**Fig. 2b**) [11]. The displacement-length ratio (*D*/*L*) decreases with increasing length, indicating that the fault aspect ratio is increasing [2,3]. The pattern of deformation, flat-topped throw distributions, and decreasing *D*/*L* suggest that these faults are restricted at depth by a mechanical boundary. Our results from boundary element modeling indicate the depth to this boundary is between 2.5 and 3 km.

Faults increase in displacement towards Alba Patera from the northern plains study area. A 500 km long fault that partially traverses this area from the northern plains has a flat-topped displacement distribution with a maximum displacement slightly over 200 m and a faulting depth of ~7 km.

**Conclusions and Implications:** We have identified what appear to be several levels of vertical restriction to the east of Alba Patera and extending across the transition to the northern plains. The northern segments of Tantalus Fossae are restricted by a mechanical/lithologic boundary 2.5-3 km deep (**Fig. 3**). We infer that this depth corresponds to the base of northern plains materials, in general agreement with depths of Frey et al. [12] based upon Quasi-Circular Depressions. South of this area, closer to Alba Patera, faulting depth increases to ~7 km. This is similar to a boundary we identify on the eastern flank of Alba Patera and it may indicate that a restricting horizon is continuous over this area. The faults in region A on Alba Patera have larger down-dip depths than those in region B and are not clearly restricted, so they have either broken through the identified boundary or the boundary is not continuous in the region.

The displacement-length ratios in region A (area one) and area two differ, with the latter having smaller *D*/*L*. Since displacement is dependent on fault geometry and material properties of the surrounding rock mass [2], we conclude that these differences are likely a result of a change in material properties between these two study areas and the restriction of the area two grabens. We observe differences in morphology (degradation) of the grabens on Alba Patera and across the transition to the northern plains, which supports our hypothesis that the change in *D*/*L* is due in part to changes in material properties since the faults are continuous across this area and are mapped to have formed during the same period of time [13]. These differences in morphology and *D*/*L* between study areas likely indicate a change in material properties and therefore could signify a difference in the formation mechanisms of the grabens.

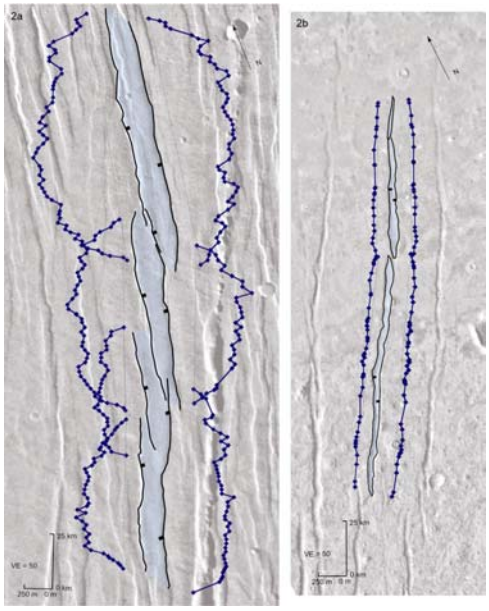


**Figure 2.** a) Throw distributions for faults from region A. Notice the scaling of displacement with fault length. b) Throw distributions for two grabens from the second study area (centered at 59°N, 273°E). Notice the small displacement relative to region A and the flat-topped displacement distributions.

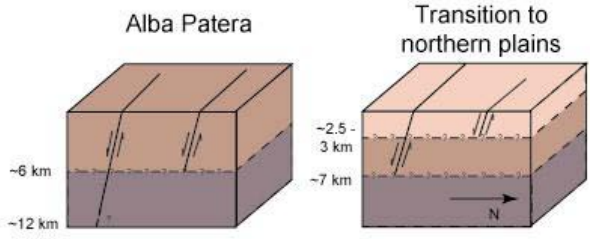


**Figure 3.** Geologic cross-sections of the two study areas showing inferred mechanical/lithologic boundaries and resulting fault restriction.

**References:** [1] Ackermann R.V. et al. (2001) *JSG, 23,* 1803-1819. [2] Schultz R.A. and Fossen H. (2002) *JSG, 24*, 1389-1411. [3] Soliva R. and Benedicto A. (2005) *JSG*, in press. [4] Plescia J.B. (1991) *JGR, 96,* 18883-18895. [5] Davis P.A. et al. (1995) *Icarus, 114,* 403-422. [6] Okubo C.H. et al. (2004) *Comp. & Geosci., 30*, 59-72. [7] Crouch S.L. and Starfield A.M. (1983) *Boundary Element Modeling in Solid Mechanics*: Unwin Hyman Inc. [8] Schultz, R.A. (1992) *Eng. Analysis with Boundary Elements, 10,* 147-154. [9] Tanaka K.L. (1990) *LPSC XX*, 515-523. [10] Bellahsen, N. et al. (2003) *JSG, 25,* 1471-1485. [11] Polit A.T. and Schultz R.A. (2004) *Eos Trans. AGU, 85*(47), Fall Meet. Suppl., T41F-1280 [12] Frey H.V. et al. (2002) *GRL, 29,* 1384, 10.1029/2001GL013832. [13] Anderson R.C. et al. (2001) *JGR, 106,* 20563-20585.

Abstract published in: Lunar and Planetary Science XXXVI, CD-ROM, Lunar and Planetary Institute, Houston (2005).